Supporting Online Material

Materials and methods

Materials Human recombinant TNFα was supplied by Calbiochem (UK). Leptomycin B was supplied by LC Laboratories (MA, USA). Tissue culture medium was supplied by Gibco Life Technologies (UK) and fetal calf serum was from Harlan Seralab (UK). All other chemicals were supplied by Sigma (UK) unless stated otherwise.

Plasmids All plasmids were propagated using *E.coli* DH5α and purified using Qiagen Maxiprep kits (Qiagen, UK). κB-Luc (pNF-κB-Luc, Stratagene, UK) contains five repeats of a κB- motif upstream of the TATA box controlling expression of luciferase. pIκBα-EGFP (Clontech, CA, USA), RelA-EGFP and RelA-DsRed and were described previously (1). RelA-DsRed-Express contains the optomised DsRed-Express fluorescent protein (Clontech, CA, USA) fused to the C-terminus of RelA. κB-IκBα-EGFP was produced by cloning a *Not*I.(filled in with T4 DNA polymerase) – *Eco*RI fragment containing the IκBα-EGFP fusion gene into the *Eco*RI and *Eco*RV sites of κB-Luc.

Cell culture HeLa (Human cervical carcinoma, ECACC No. 93021013) and SK-N-AS (human S-type neuroblastoma, ECACC No. 94092302) cells were grown in Minimal Essential Medium with Earle's salts plus 10% fetal calf serum and 1% non-essential amino acids and maintained at 37°C, 5% CO_2. For confocal fluorescence microscopy and luminescence microscopy, HeLa or SK-N-AS cells were plated on 35 mm glass-bottom dishes (Iwaki, Japan) at $2.4x10^4$ cells and $1x10^5$ cells respectively per dish in 3 ml medium. 24 h post-transfection, the cells were transfected with the appropriate plasmid(s) using Fugene 6 (Boehringer Mannheim/Roche, Germany) in accordance with the manufacturer's recommendations. The optimised ratio of DNA:Fugene 6 used for transfection of HeLa or SK-N-AS cells was 1 μg DNA with 2 μl Fugene 6 and 0.8 μg DNA with 1.2 μl Fugene 6 respectively. For Western blotting, HeLa or SK-N-AS cells were plated on 60 mm tissue culture dish (Iwaki, Japan) at $3x10^5$ and $1x10^6$ cells respectively per dish in 5 ml medium. For immunocytochemistry, HeLa cells were plated in Lab-Tek 8-well chamber slides from Nalge Nunc International (IL, USA) at 2.4×10^3 cells per well in 400 μl medium.

Treatment of cells with TNFα, etoposide and leptomycin B 48 h post transfection cells were treated with either TNFα (10 ng/ml), etoposide (20 μM) or leptomycin B (18 nM, in addition to 10 ng/ml TNFα) by replacing one tenth of the media volume in the dish with the appropriate solution. For experiments using continual TNFα stimulation the TNFα-containing medium was left on the cells for the duration of the experiment. For TNFα pulse experiments, the cells were stimulated with 10 ng/ml TNFα for 5mins and then washed 3 times with fresh medium. The cells were imaged either immediately after treatment or incubated (at 37°C, 5% CO_2) for the indicated duration prior to cell lysis or fixation.

Western blotting Whole cell lysates were prepared at the indicated times after stimulation. Proteins were separated by polyacrylamide gel (10%) electrophoresis then transferred to nitrocellulose membranes. Membranes were probed using the following antibodies: anti-IκBα (#9242, Cell Signaling, MA, USA), anti-phospho-IκBα (Ser 32) (#9241, Cell Signaling, MA, USA), anti-RelA (#3034, Cell Signaling, MA, USA) and anti-phospho-RelA (#3031, Cell Signaling, MA, USA). For relative quantification of protein levels lysates were produced in triplicate for blotting. Band intensity was quantified using a BioRad GS-710 Densitometer and Quantity One software (Version 4.5.0).

Immunocytochemistry Cells were fixed with methanol for 6 min at 20°C at the times indicated following stimulation. They were then washed 3 times with PBS and then blocked in PBS supplemented with 1% BSA. The cells were incubated with anti-RelA sc-109 antibodies from Santa Cruz (CA, USA) at a 1:100 dilution in PBS supplemented with 1% BSA for 60 min at room temperature and then washed 3 times with PBS supplemented with 1% BSA for 10 min. The cells were washed 3 times in PBS supplemented with 1% BSA and then incubated with anti-rabbit IgG Cy3 conjugate (Sigma, UK) at a 1:100 dilution in PBS supplemented with 1% BSA for 30 min. The cells were washed 3 times in PBS supplemented with 1% BSA then once with PBS. Vectorshield from Vector Laboratories Inc. (CA, USA) and a coverslip were applied to the slides before imaging.

Fluorescence microscopy Confocal microscopy was carried out on transfected cells in 35mm glass bottom dishes in a humidified CO_2 incubator (at 37°C, 5% CO_2) using a Zeiss Axiovert 200 with a 40x phase contrast oil immersion objective (NA =1.3). Excitation of EGFP was performed using an Argon ion laser at 488nm. Emitted light was reflected through a 505-550nm bandpass filter from a 540nm dichroic mirror. DsRed and DsRed-Express fluorescence was excited using a green Helium Neon laser (543nm) and detected through a 570nm long-pass filter. Microscopy was carried out on slides of fixed cells using a Zeiss LSM510 with a 40x phase contrast oil immersion objective (numerical aperture=1.3). Excitation of CY3 was performed using a green Helium Neon laser (543nm). Emitted light was reflected through a 560nm long-pass filter from a 545nm dichroic mirror. Data capture and extraction was carried out with LSM510 version 3.0 software (Zeiss, Germany). For IκBα fusion proteins, integrated cellular fluorescence intensities were calculated for each cell at time=0 using AQM Advance 6.0 software (Kinetic Imaging, UK). For RelA fusion proteins, mean fluorescence intensities were calculated for each time point for both nuclei and cytoplasm then nuclear:cytoplasmic (N:C) fluorescence intensity ratios were determined. For figures 2A-F, amplitude is expressed as N:C fluorescence intensity normalised to the average amplitude for that population of cells. For figure 4B, amplitude is expressed as nuclear DsRed fluorescence relative to maximum nuclear fluorescence for each cell normalised to 100.

Luminescence microscopy Luminescence imaging was carried out on pNF-κB-Luc transfected cells in 35 mm glass bottom dishes in a humidified CO_2 incubator (at 37°C, 5% CO_2) using a Hamamatsu VIM photon counting camera attached to the Keller port of a

Zeiss Axiovert 135 TV with a 20x FLUAR objective (NA=1.3). Prior to imaging, cells were incubated on the microscope stage for 2 h at 37°C, 5% CO_2 in the presence of 1mM luciferin (Biosynth AG, Switzerland). Argus-20 control program version 3.53 software (Hamamatsu Photonics K. K, Japan) was used for image acquisition, AQM Advance 6.0 software (Kinetic Imaging, UK) was used for image analysis. Images were acquired using 30 min integration times. For figures 2G-K and 4C, amplitude is expressed as the mean of cellular luminescence.

Mathematical modeling All simulations were performed using the simulator Gepasi (3), initially with the parameters described in the revised supplementary information for Hoffmann *et al* (2002) (http://www.sciencemag.org/cgi/data/298/5596/1241/DC1/2), including the pre-equilibration period of 2000s. A diagram of the network (Fig S1) and the reaction numbers (Table S1) are given below. Parameters were varied using the 'scan' function in Gepasi.

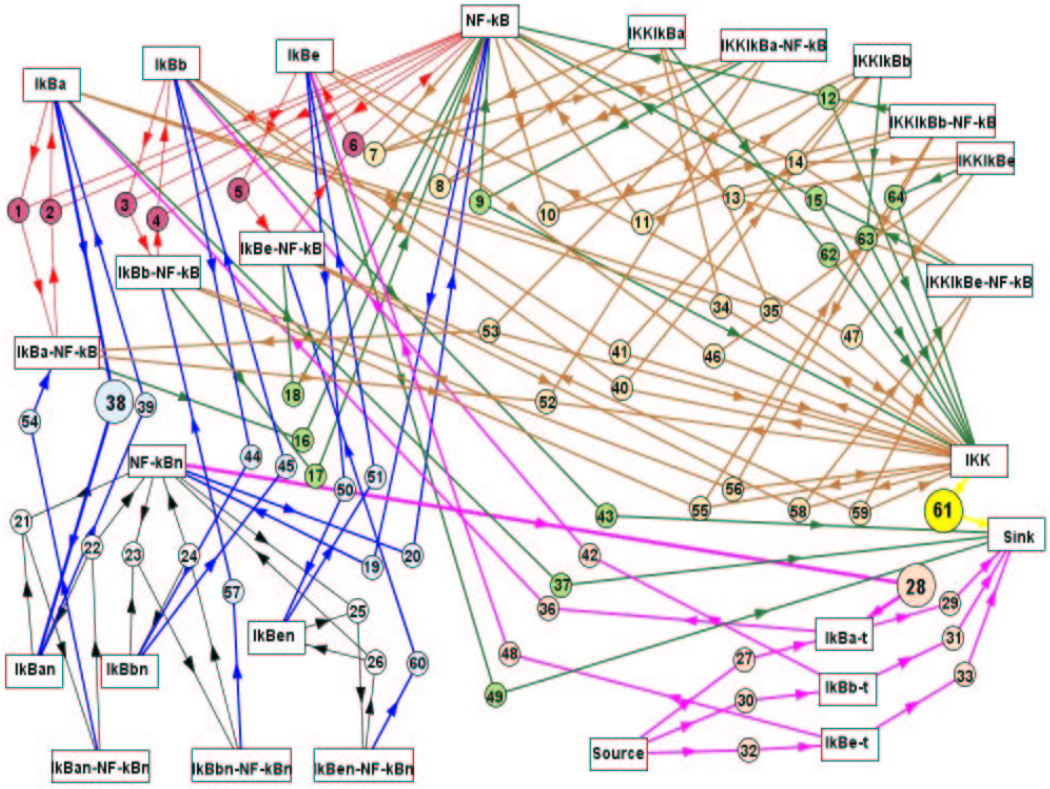

Figure S1: Network diagram showing individual reactions included in the computational model (2). *See table S1 for identity of individual reactions and rate constants.*

	Reactions	Symbol	Values	Units (mins)
1	IκBα + NF-κB → IκBα-NF-κB	k_{a4}	30	$\mu M^{-1}min^{-1}$
2	IκBα-NF-κB → NF-κB + IκBα	k_{d4}	0.03	min^{-1}
3	IκBβ + NF-κB → IκBβ-NF-κB	k_{a5}	30	$\mu M^{-1}min^{-1}$
4	IκBβ-NF-κB → NF-κB + IκBβ	k_{d5}	0.03	min^{-1}
5	IκBε + NF-κB → IκBε-NF-κB	k_{a6}	30	$\mu M^{-1}min^{-1}$
6	IκBε-NF-κB → NF-κB + IκBε	k_{d6}	0.03	min^{-1}
7	IKKIκBα + NF-κB → IKKIκBα-NF-κB	k_{a4}	30	$\mu M^{-1}min^{-1}$
8	IKKIκBα-NF-κB → NF-κB + IKKIκBα	k_{d4}	0.03	min^{-1}
9	IKKIκBα-NF-κB → IKK + NF-κB	k_{r4}	1.221	min^{-1}
10	IKKIκBβ + NF-κB → IKKIκBβ-NF-κB	k_{a5}	30	$\mu M^{-1}min^{-1}$
11	IKKIκBβ-NF-κB → NF-κB + IKKIκBβ	k_{d5}	0.03	min^{-1}
12	IKKIκBβ-NF-κB → IKK + NF-κB	k_{r5}	0.45	min^{-1}
13	IKKIκBε + NF-κB → IKKIκBε-NF-κB	k_{a6}	30	$\mu M^{-1}min^{-1}$
14	IKKIκBε-NF-κB → NF-κB + IKKIκBε	k_{d6}	0.03	min^{-1}
15	IKKIκBε-NF-κB → IKK + NF-κB	k_{r6}	0.66	min^{-1}
16	IκBα-NF-κB → NF-κB	$k_{deg\ 4}$	0.00135	min^{-1}
17	IκBβ-NF-κB → NF-κB	$k_{deg\ 4}$	0.00135	min^{-1}
18	IκBε-NF-κB → NF-κB	$k_{deg\ 4}$	0.00135	min^{-1}
19	NF-κB → $NF\text{-}\kappa B_n$	k_1	5.4	min^{-1}
20	$NF\text{-}\kappa B_n$ → NF-κB	k_{01}	0.0048	min^{-1}
21	$I\kappa B\alpha_n$ + $NF\text{-}\kappa B_n$ → $I\kappa B\alpha_n$-$NF\text{-}\kappa B_n$	k_{a4}	30	$\mu M^{-1}min^{-1}$
22	$I\kappa B\alpha_n$-$NF\text{-}\kappa B_n$ → $NF\text{-}\kappa B_n$ + $I\kappa B\alpha_n$	k_{d4}	0.03	min^{-1}
23	$I\kappa B\beta_n$ + $NF\text{-}\kappa B_n$ → $I\kappa B\beta_n$-$NF\text{-}\kappa B_n$	k_{a5}	30	$\mu M^{-1}min^{-1}$
24	$I\kappa B\beta_n$-$NF\text{-}\kappa B_n$ → $NF\text{-}\kappa B_n$ + $I\kappa B\beta_n$	k_{d5}	0.03	min^{-1}

25	$I\kappa B\varepsilon_n + NF\text{-}\kappa B_n \rightarrow I\kappa B\varepsilon_n\text{-}NF\text{-}\kappa B_n$	k_{a6}	30	$\mu M^{-1}min^{-1}$
26	$I\kappa B\varepsilon_n\text{-}NF\text{-}\kappa B_n \rightarrow NF\text{-}\kappa B_n + I\kappa B\varepsilon_n$	k_{d6}	0.03	min^{-1}
27	source $\rightarrow I\kappa B\alpha\text{-}_t$	k_{tr2a}	9.21375e-5	$\mu M^{-1}min^{-1}$
28	$NF\text{-}\kappa B_n + NF\text{-}\kappa B_n \rightarrow I\kappa B\alpha_t + NF\text{-}\kappa B_n + NF\text{-}\kappa B_n$	k_{tr2}	1.027125	$\mu M^{-1}min^{-1}$
29	$I\kappa B\alpha\text{-}_t \rightarrow$ sink	k_{tr3}	0.0168	min^{-1}
30	source $\rightarrow I\kappa B\beta\text{-}_t$	k_{tr2b}	1.0701e-5	$\mu M^{-1}min^{-1}$
31	$I\kappa B\beta\text{-}_t \rightarrow$ sink	k_{tr3}	0.0168	min^{-1}
32	source $\rightarrow I\kappa B\varepsilon\text{-}_t$	k_{tr2e}	7.644e-6	$\mu M^{-1}min^{-1}$
33	$I\kappa B\varepsilon\text{-}_t \rightarrow$ sink	k_{tr3}	0.0168	min^{-1}
34	$IKK + I\kappa B\alpha \rightarrow IKKI\kappa B\alpha$	k_{a1}	1.35	$\mu M^{-1}min^{-1}$
35	$IKKI\kappa B\alpha \rightarrow IKK + I\kappa B\alpha$	k_{d1}	0.075	min^{-1}
36	$I\kappa B\alpha\text{-}_t \rightarrow I\kappa B\alpha + I\kappa B\alpha\text{-}_t$	k_{tr1}	0.2448	min^{-1}
37	$I\kappa B\alpha \rightarrow$ sink	$k_{deg\,1}$	0.00675	min^{-1}
38	$I\kappa B\alpha \rightarrow I\kappa B\alpha_n$ (Import)	k_{tp1}	0.018	min^{-1}
39	$I\kappa B\alpha_n \rightarrow I\kappa B\alpha$ (Export)	k_{tp2}	0.012	min^{-1}
40	$IKK + I\kappa B\beta \rightarrow IKKI\kappa B\beta$	k_{a2}	0.36	$\mu M^{-1}min^{-1}$
41	$IKKI\kappa B\beta \rightarrow IKK + I\kappa B\beta$	k_{d2}	0.105	min^{-1}
42	$I\kappa B\beta\text{-}_t \rightarrow I\kappa B\beta + I\kappa B\beta\text{-}_t$	k_{tr1}	0.2448	min^{-1}
43	$I\kappa B\beta \rightarrow$ sink	$k_{deg\,1}$	0.00675	min^{-1}
44	$I\kappa B\beta \rightarrow I\kappa B\beta_n$ (Import)	0.5 k_{tp1}	0.009	min^{-1}
45	$I\kappa B\beta_n \rightarrow I\kappa B\beta$ (Export)	0.5 k_{tp2}	0.006	min^{-1}
46	$IKK + I\kappa B\varepsilon \rightarrow IKKI\kappa B\varepsilon$	k_{a3}	0.54	$\mu M^{-1}min^{-1}$
47	$IKKI\kappa B\varepsilon \rightarrow IKK + I\kappa B\varepsilon$	k_{d3}	0.105	min^{-1}
48	$I\kappa B\varepsilon\text{-}_t \rightarrow I\kappa B\varepsilon + I\kappa B\varepsilon\text{-}_t$	k_{tr1}	0.2448	min^{-1}
49	$I\kappa B\varepsilon \rightarrow$ sink	$k_{deg\,1}$	0.00675	min^{-1}
50	$I\kappa B\varepsilon \rightarrow I\kappa B\varepsilon_n$ (Import)	0.5 k_{tp1}	0.009	min^{-1}
51	$I\kappa B\varepsilon_n \rightarrow I\kappa B\varepsilon$ (Export)	0.5 k_{tp2}	0.006	min^{-1}

52	IKK + IκBα-NF-κB → IKKIκBα-NF-κB	k_{a7}	11.1	$\mu M^{-1}min^{-1}$
53	IKKIκBα-NF-κB → IKK + IκBα-NF-κB	k_{d1}	0.075	min^{-1}
54	$I\kappa B\alpha_n$-NF-κB_n → IκBα-NF-κB (Export)	k_2	0.82944	min^{-1}
55	IKK + IκBβ-NF-κB → IKKIκBβ-NF-κB	k_{a8}	2.88	$\mu M^{-1}min^{-1}$
56	IKKIκBβ-NF-κB → IKK + IκBβ-NF-κB	k_{d2}	0.105	min^{-1}
57	$I\kappa B\beta_n$-NF-κB_n → IκBβ-NF-κB (Export)	0.4 k_2	0.31187	min^{-1}
58	IKK + IκBε-NF-κB → IKKIκBε-NF-κB	k_{a9}	4.2	$\mu M^{-1}min^{-1}$
59	IKKIκBε-NF-κB → IKK + IκBε-NF-κB	k_{d3}	0.105	min^{-1}
60	$I\kappa B\varepsilon_n$-NF-κB_n → IκBε-NF-κB (Export)	0.4 k_2	0.31187	min^{-1}
61	IKK → sink	k_{02}	0.0072	min^{-1}
62	IKKIκBα → IKK	k_{r1}	0.2442	min^{-1}
63	IKKIκBβ → IKK	k_{r2}	0.09	min^{-1}
64	IKKIκBε → IKK	k_{r3}	0.132	min^{-1}

Table S1: Summary of parameter values in form of reaction rate constants included in the computational model.

Supporting data

Section A: Functionality of fluorescent fusion constructs and control experiments

The transcriptional functionality of the RelA fluorescent fusions (RelA-DsRed and RelA-EGFP) have been demonstrated in our previous work (1). One recent study (3) has provided further information relating the function of fluorescent RelA and IκBα fusion proteins to the processing of the endogenous proteins. These studies show that expression levels of the fusion proteins can change the kinetics of the system through changes in protein concentration, but do not affect the fundamental characteristics of NF-κB signaling. Indeed, the use of quantifiable additional expression of these proteins has been a very useful tool for the analysis of how differing expression levels affect the signaling kinetics.

In the initial experiments performed in this study the cells were transfected with both RelA-DsRed and IκBα-EGFP, since our previous studies in HeLa cells (2) had suggested that dual transfection of these fusion proteins gave rise to dynamics of their processing in response to TNFα stimulation that was closest to that of the endogenous proteins in untransfected cells. Two issues that could affect the present results, might therefore be the effect of overexpression of these proteins and the possible effect of fluorescent protein fusion on RelA and IκBα protein function.

We estimate that the fluorescent fusion proteins may be expressed at a level of approximately 3 – 5 fold over that of the endogenous proteins (3 & data not shown) when expressed from the hCMV promoter. When the starting level of NF-κB (equivalent to RelA) was increased by 4-fold in the computational model, it had a negligible effect on the fundamental characteristics of NF-κB N:C oscillations.

Using dual transfection of RelA-DsRed and RelA-EGFP into SK-N-AS cells, fluorescence from the different fusion proteins showed almost identical translocation dynamics in response to TNFα (Fig. S2A-B). These data demonstrate that both the DsRed and EGFP fusion proteins showed the same functional behavior. (Similar data was obtained for the Rel-A DsRed-Express fusion protein, data not shown). These data provide further support that the addition of different fusion partners to RelA does not significantly affect its function.

When either HeLa cells or SK-N-AS cells were expressing EGFP alone, no oscillations in nuclear-cytoplasmic (N-C) localization were ever observed, before or after TNFα treatment. When cells were expressing the RelA fluorescent fusion proteins, N:C oscillations were seen extremely rarely in untreated cells. Under the microscopy conditions used (minimal laser illumination), the level of photobleaching of any of the fluorescent proteins was insignificant during the timecourse of the imaging experiments.

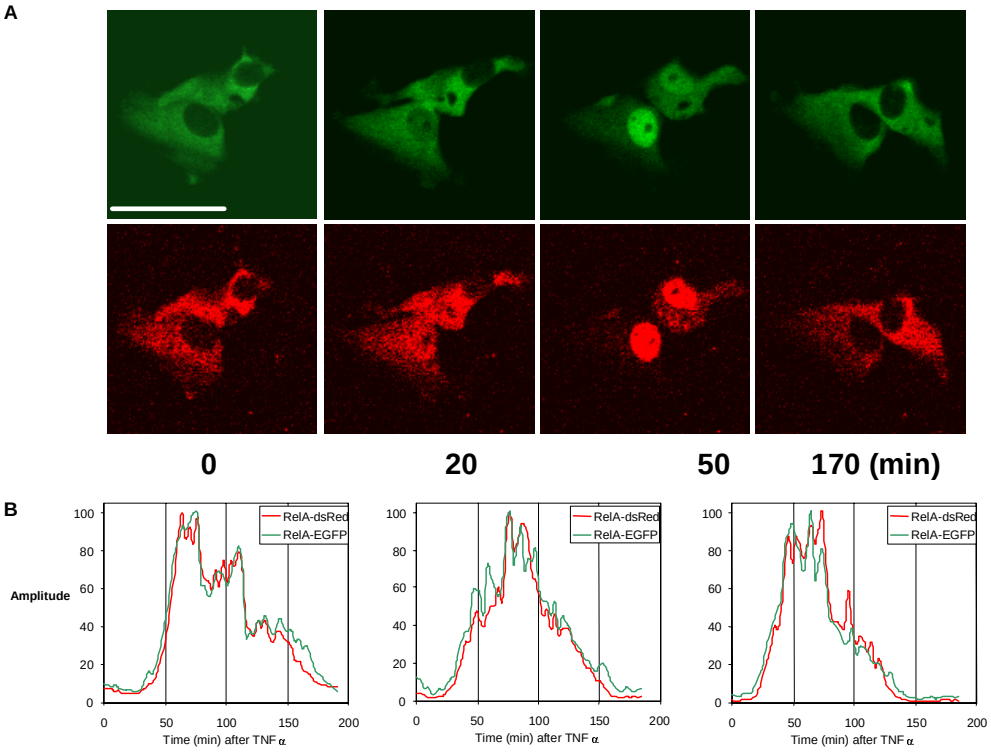

Figure S2: Comparison of RelA-DsRed and RelA-EGFP dynamics in response to continual TNFα stimulation. *SK-N-AS cells were transfected with RelA-DsRed (red) and RelA-EGFP (green). 48 h post-transfection, cells were stimulated with 10 ng/ml TNFα.* ***A.*** *Two color confocal images (DsRed=red, EGFP=green) were collected at 3 min intervals for 170 min.* ***B.*** *3 individual cells were analysed for RelA-DsRed and RelA-EGFP N:C ratio at each time point. Fluorescence from each protein was normalised to the maximum during the experiment (100%).*

Section B: Immunocytochemistry analysis of endogenous RelA localization in response to TNFα To determine whether endogenous RelA displays oscillatory behavior, the localization of endogenous RelA in response to TNFα was assessed using immunocytochemistry. Non-transfected HeLa cells were treated with TNFα for periods up to 180 min. At the times indicated, cells were methanol fixed and incubated with rabbit anti-RelA followed by an anti-rabbit IgG Cy3 conjugated secondary antibody. Fluorescence was then visualised using the Zeiss Axiovert 200 system (see materials and methods). Individual images were randomised then scored by eye as the number of cells/field where nuclear fluorescence<cytoplasmic fluorescence (N<C), nuclear fluorescence=cytoplasmic fluorescence (N=C) or nuclear fluorescence>cytoplasmic fluorescence (N>C).

Graphical analysis of these data highlights not only an initial shift of RelA from the cytoplasm to the nucleus, returning predominantly to the cytoplasm by 90 minutes following TNFα treatment, but a subsequent nuclear entry of RelA by 180 minutes post-stimulation. These data provide further evidence of the biphasic response demonstrated by the use of fluorescent fusion proteins and western blotting, supporting the theory that sustained stimulation generates oscillations in endogenous NF-κB localization.

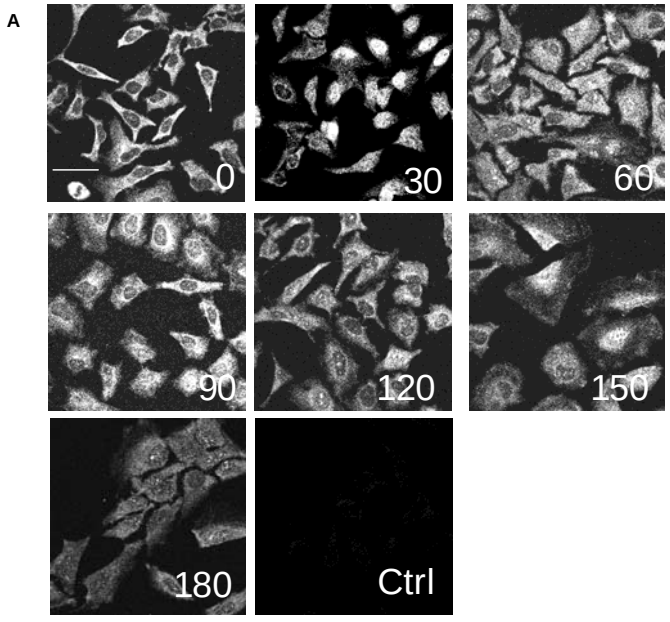

C

Time	N<C	N>C	N=C
0	100	0	0
30	16.2	44.7	39.1
60	54.5	16.9	28.6
90	89.6	4.5	5.9
120	94.6	1.2	4.1
150	82.7	5.6	11.7
180	58.5	9.1	32.4

Figure S3: Immunocytochemistry analysis of endogenous RelA localization after TNFα stimulation *A.* *Images of RelA localization in fields of HeLa cells at the indicated times.* ***B.*** *Percentage of cells (+/- SEM) showing nuclear or equal nuclear and cytoplasmic RelA localization.* ***C.*** *Data showing percentage of cells with nuclear, cytoplasmic or equal nuclear and cytoplasmic RelA localization at different time intervals (min) following TNFα stimulation. Scale bar represents 50 μm.*

Section C: Western blot analysis of IκBα and RelA protein and phosphoprotein levels. We investigated the relationship between the observed dynamics of N:C oscillations and NF-κB-dependent transcription (see Fig. 2) and the timing of endogenous RelA phosphorylation (at Ser536 (4, 5)), IκBα phosphorylation (Ser32 (6)) and IκBα degradation. Western blot analysis showed that in both SK-N-AS (see Fig. 4D) and HeLa cells (Fig. S4A) treated with constant TNFα, there was a biphasic pattern in the time-course of Ser32 phospho-IκBα and Ser536 phospho-RelA levels. In HeLa cells the phosphoprotein levels appeared to diminish more rapidly. Western blot analysis of HeLa cells (or SK-N-AS cells, data not shown) treated with a 5 min pulse of TNFα (Fig. S4B) showed a single transient increase in Ser32 phospho-IκBα levels and a single phase of Ser536 phospho-RelA accumulation that decreased within 30 min. Western blot analysis of SK-N-AS cells treated with the topoisomerase II inhibitor etoposide (VP16) Ser32 phospho-IκBα levels and Ser536 phospho-RelA levels (Fig. S4C) showed that these phosphoproteins appeared together at ~120 min (with a clear biphasic pattern for IκBα) and subsequently decreased.

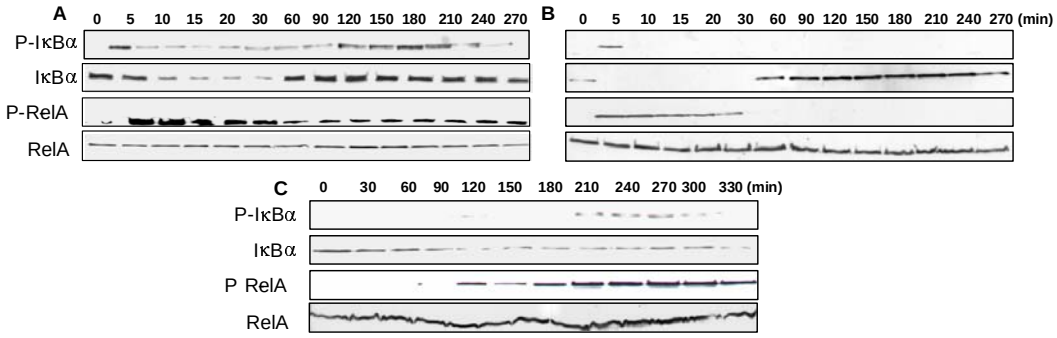

Figure S4: Western blot analysis of IκBα and RelA total and phosphoprotein levels (P-IκBα and P-RelA) in HeLa and SK-N-AS cells. ***A.*** *HeLa cells treated with continual 10 ng/ml TNFα.* ***B.*** *HeLa cells treated with a 5 min pulse of 10 ng/ml TNFα and then TNFa free medium.* ***C.*** *SK-N-AS cells treated with continual 20 μM etoposide. Times indicate the time of analysis following stimulation. (P-IkBa = Ser32 phospho-IkBa. P-RelA = Ser536 phospho-RelA.)*

In order to quantify the persistence of the IκBα and RelA phosphoprotein levels we prepared triplicate sets of lysates from SK-N-AS and HeLa cells at 0 min, 5 min and 20 h post-TNFα stimulation (Fig. S5). These lysates were each analysed by western blotting and densitometry to measure total IκBα levels (Fig. S5A) Ser32 phospho-IκBα levels (Fig. S5B) and Ser536 phospho-RelA levels (Fig. S5C).

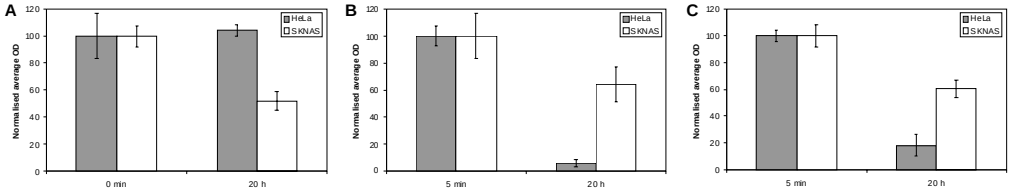

Figure S5: Quantification of total IκBα, phospho-IκBα and phospho-RelA levels. *HeLa and SK-N-AS cells were analysed for **A**. Total IκBα. **B.** Ser32 phospho-IκBα. **C.** Ser536 phospho-RelA. Triplicate lysates were analysed at 0 min, 5 min and 20 h after continual TNFα stimulation. Total IκBα levels at 20 h are shown relative to the maximum at 0 min. Phospho-IκBα and phospho-RelA levels at 20 h are shown relative to the maximum at 5 min (with background at 0 min subtracted). (Error bars represent S.D.)*

Section D: Images of RelA-DsRed plus IκBα-EGFP or EGFP in SK-N-AS and HeLa cells and luminescence images of κB promoter-directed luciferase expression, following various treatments (as described in figure 2).

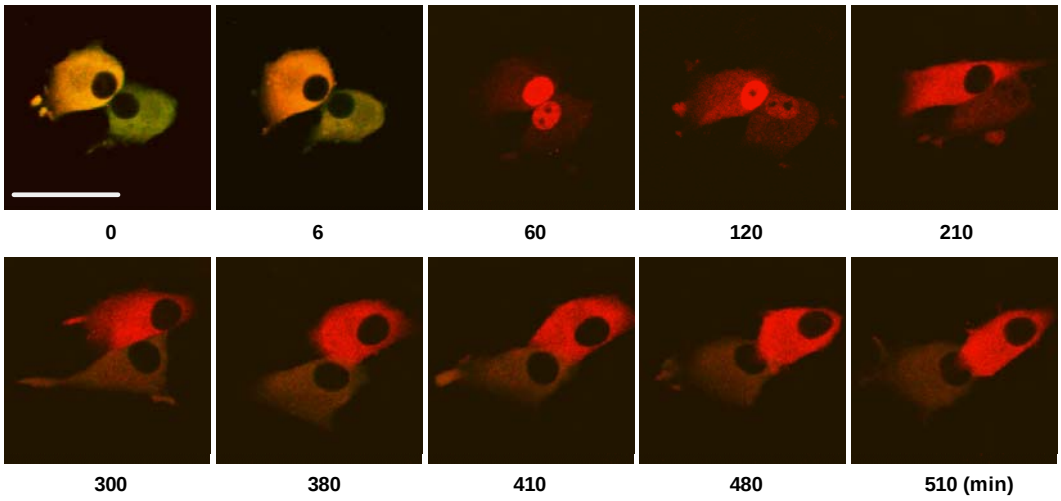

Figure S6: Time-course images of RelA-DsRed (red) and IκBα-EGFP (green) expressing SK-N-AS cells stimulated with a 5 min pulse of 10 ng/ml TNFα. *Images relate to data in Figure 2B. Scale bar represents 50 μm.*

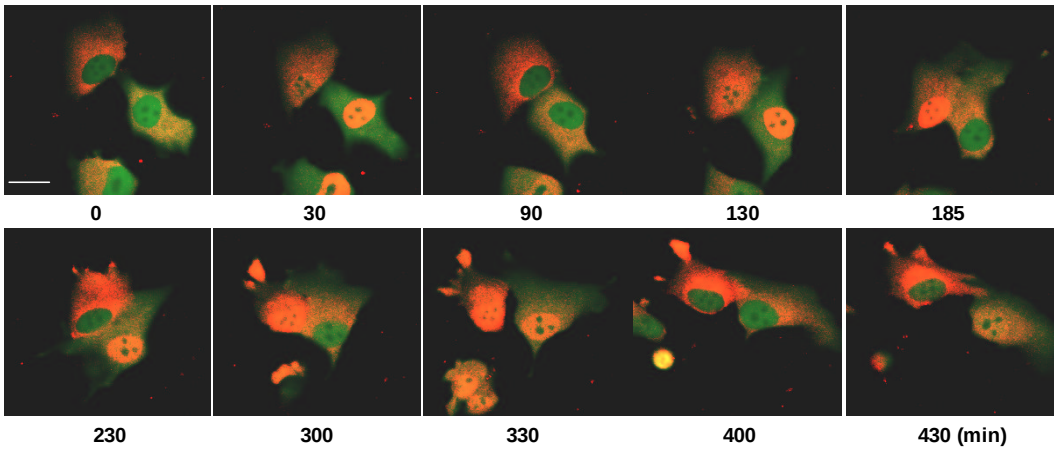

Figure S7: Time-course images of RelA-DsRed (red) and EGFP (green) expressing SK-N-AS cells stimulated with continual 10 ng/ml TNFα. *Images relate to data in Figure 2C. Scale bar represents 20 μm.*

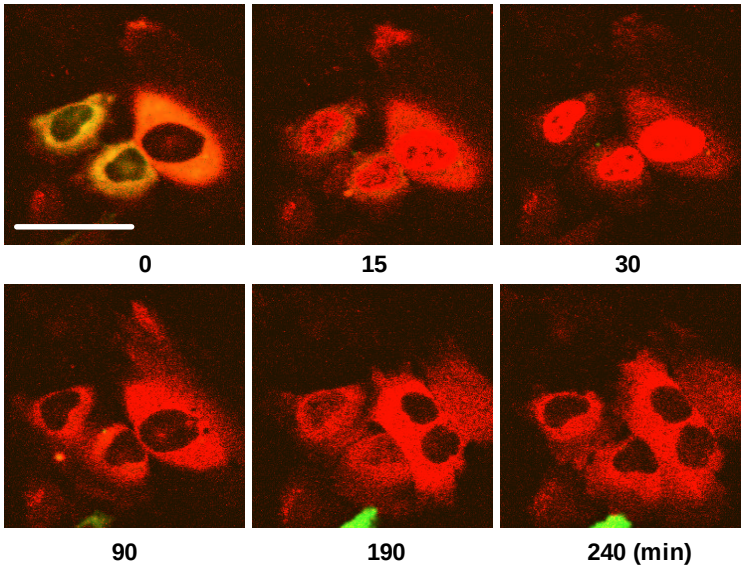

Figure S8: Time-course images of RelA-DsRed (red) and IκBα-EGFP (green) expressing HeLa cells stimulated with continual 10 ng/ml TNFα. *Images relate to data in Figure 2D. Scale bar represents 50 μm.*

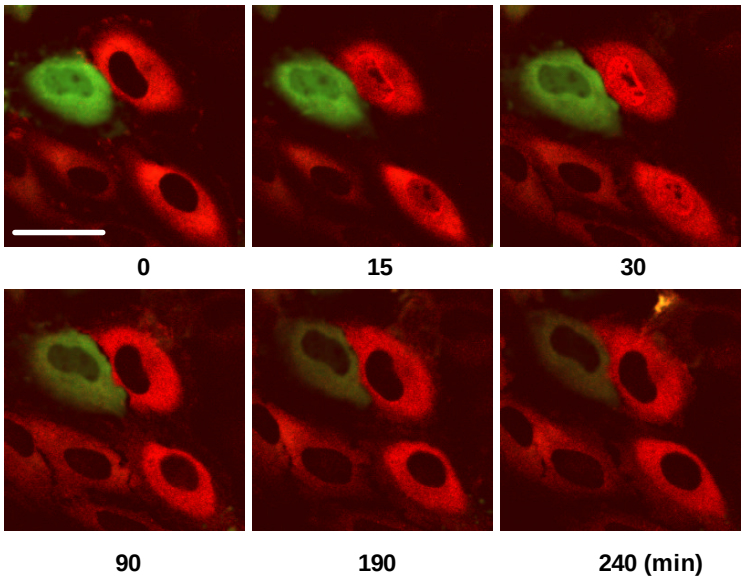

Figure S9: Time-course images of RelA-DsRed (red) and IκBα-EGFP (green) expressing HeLa cells stimulated with a 5 min pulse of TNFα. *Images relate to data in Figure 2E. Scale bar represents 50 μm.*

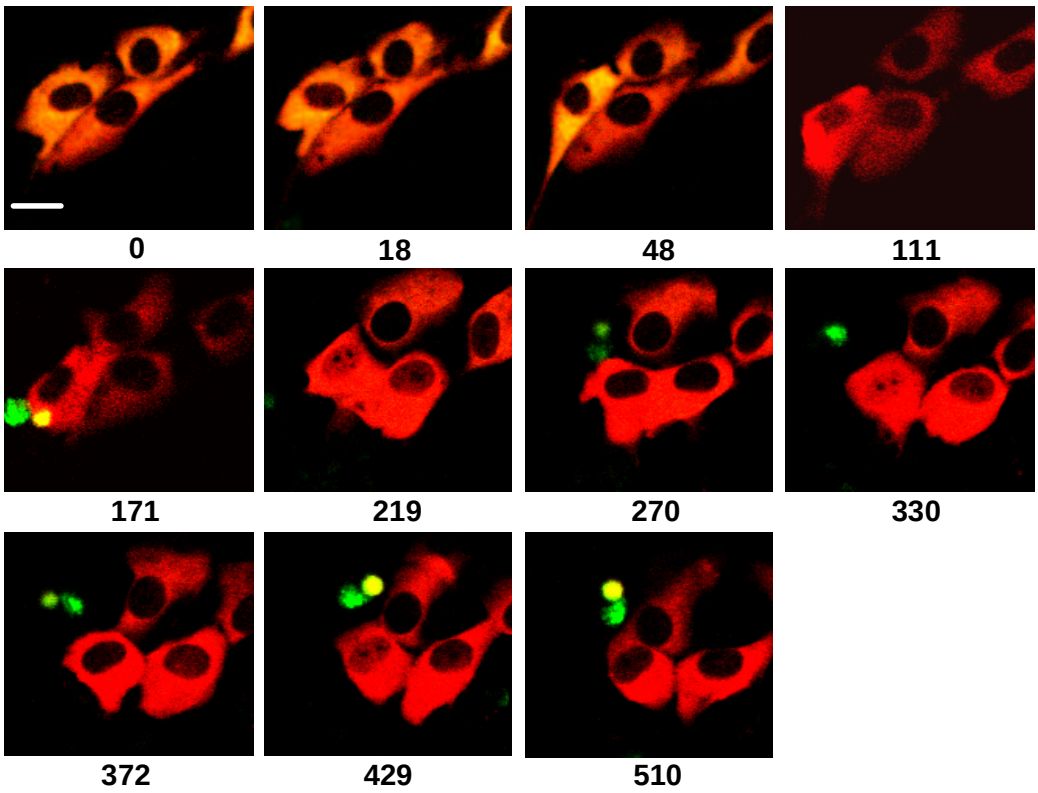

Figure S10: Time-course images of RelA-DsRed (red) and IκBα-EGFP (green) expressing SK-N-AS cells stimulated with 20 μM etoposide. *Images relate to data in Figure 2F. Scale bar represents 20 μm.*

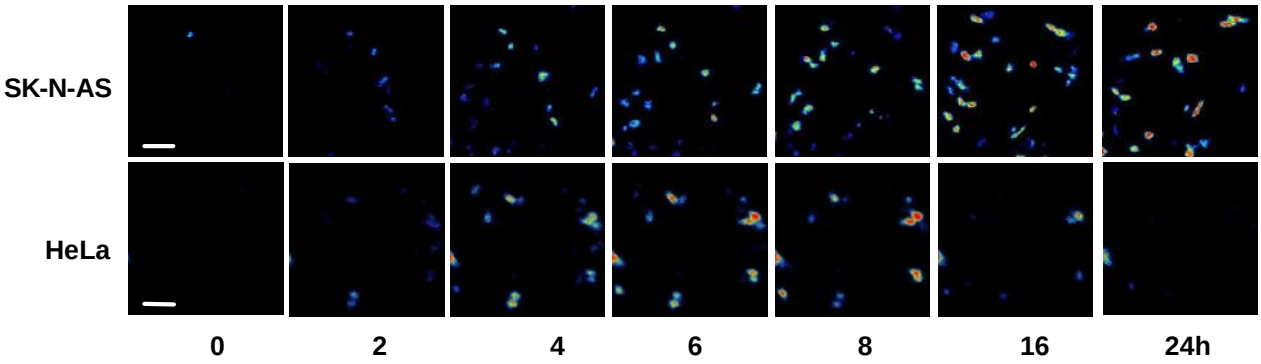

Figure S11: Luminescence imaging (photon counts) of the dynamics of NF-κB-dependent luciferase reporter gene activity in SK-N-AS and HeLa cells following continual TNFα stimulation. Images relate to data in Fig. 2G & I respectively. Scalebar represents 100 μm. Colour represents intensity increasing from blue through yellow to red.

Section E: Analysis of N:C oscillations in RelA-EGFP- and RelA-DsRed-expressing SK-N-AS cells.

SK-N-AS cells expressing RelA-EGFP displayed N:C oscillations of similar period and damping to RelA-DsRed expressing SK-N-AS cells (see Fig. 2C & S14). 86% of 110 cells responded to TNFα and 74% of cells showed oscillations in RelA localization.

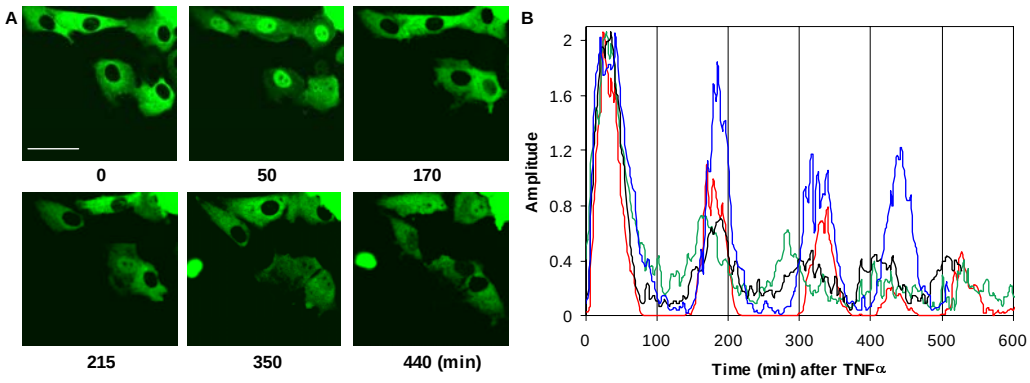

Figure S12: RelA-EGFP N:C oscillations in SK-N-AS cells stimulated with continual 10 ng/ml TNFα. *SK-N-AS cells were transfected with RelA-EGFP. 24 h post transfection, cells were stimulated with 10 ng/ml TNFα.* ***A.*** *Single color confocal images of RelA-EGFP (green) expressing SK-N-AS stimulated with TNFα. Scale bar represents 50 μm.* ***B.*** *Analysis of 4 typical cells displaying RelA-EGFP N:C oscillations. Amplitude is expressed as the N:C ratio of EGFP fluorescence at each time-point.*

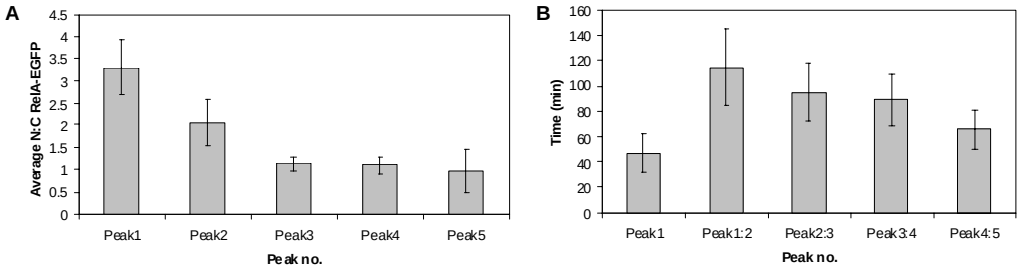

Figure S13: Period and amplitude analysis of RelA-EGFP N:C oscillations in SK-N-AS cells treated with continual 10 ng/ml TNFα. ***A.*** *Amplitude (N:C ratio) of successive oscillations in SK-N-AS cells transfected with RelA-EGFP and stimulated with TNFα (n=27 cells from 4 experiments +/- SEM).* ***B.*** *Average timing between successive peaks (+/- SEM) in SK-N-AS cells transfected with RelA- EGFP and stimulated with continual TNFα (n=27 cells from 4 experiments).*

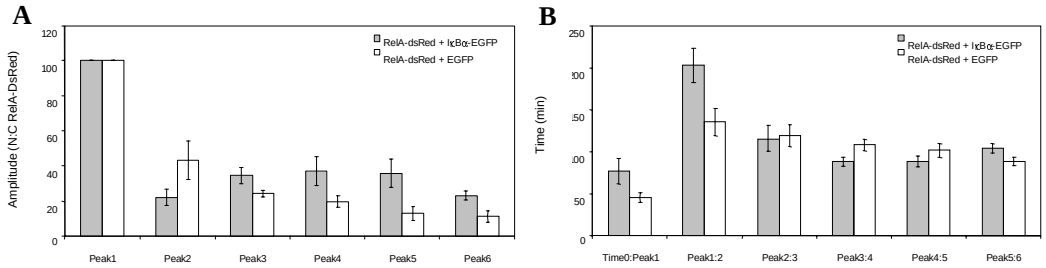

Figure S14: Period and amplitude analysis of RelA-DsRed N:C oscillations in SK-N-AS cells transfected with either hCMV-IκBα-EGFP or the control hCMV-EGFP and treated with continual 10ng/ml TNFα.

A. *Relative amplitude (N:C ratio) of successive oscillations in SK-N-AS cells transfected with RelA-DsRed and hCMV-IκBα-EGFP, or hCMV-EGFP and stimulated with TNFα. (n = 31 cells from 5 experiments and 24 cells from 3 experiments respectively, peak 1 set to 100% for each, subsequent peaks show relative amplitude +/- SEM).* ***B.*** *Average timing between successive peaks (+/- SEM) in SK-N-AS cells transfected with RelA-DsRed and hCMV-IκBα-EGFP or hCMV-EGFP and stimulated with TNFα (n = 31 cells from 5 experiments and 24 cells from 3 experiments respectively).*

Analysis of the averaged relative amplitudes and timing of successive peaks of RelA-DsRed nuclear occupancy in SK-N-AS cells showed that N:C oscillation damping (Fig. S14A) and successive peak timing (Fig. S14B) were again highly reproducible. The co-expression of IκBα-EGFP under the hCMV promoter significantly and reproducibly affected the timing (Fig. S14B) of peaks 1 and 2 (but not peak 3 onwards, since built-up IκBα-EGFP might be expected to have most effect immediately after TNFα stimulation). Peak 2 was significantly later in IκBα-EGFP-co-expressing cells. Analysis of the amplitude and level of damping of N:C oscillations in SK-N-AS cells (Fig. S14A) revealed that cells expressing RelA-DsRed (plus control vector) showed a regular pattern of damping between successive peaks, but when co-expressing IκBα-EGFP, a more complex pattern of peak

amplitude was observed. In addition, peak 1 N:C fluorescence ratio was higher in the presence of IκBα-EGFP (15.7 +/- 3.9, S.E.M.) than in cells expressing RelA-DsRed alone (5.5 +/- 1.1, S.E.M.) These observations suggested that the rate of IκBα synthesis was important in regulating both the amplitude and period of N:C oscillations (see Fig. 3 for data from HeLa cells expressing IκBα fluorescent fusion protein under the control of the NF-κB regulated promoter).

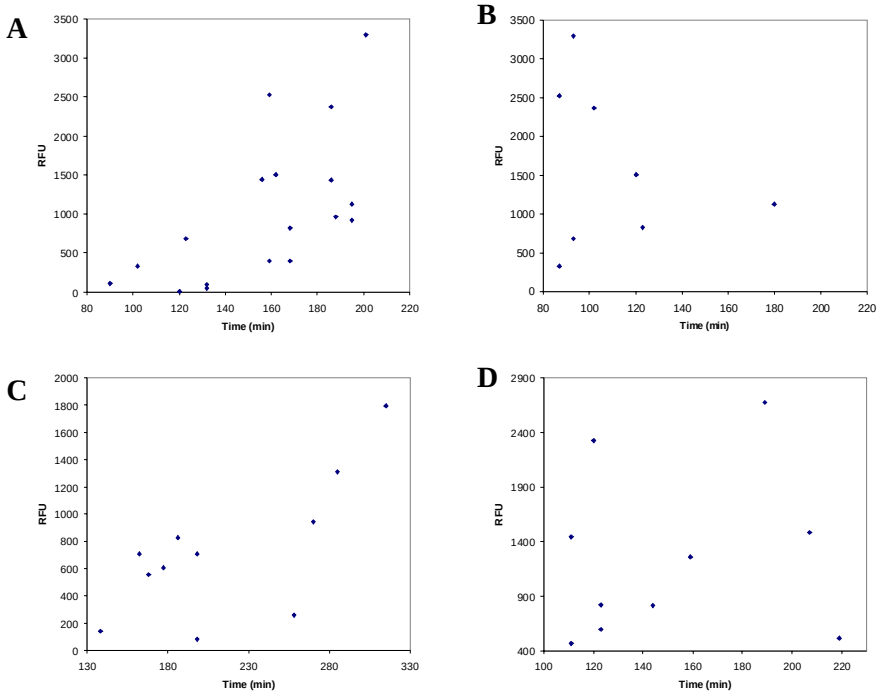

Figure S15: Effect of varying levels of IκBα-EGFP expression on TNFα stimulated N:C RelA oscillation timing in SK-N-AS and HeLa cells following stimulation with continual 10 ng/ml TNFα.
A-B. *HeLa cells co-expressing RelA-DsRed and hCMV-IκBα-EGFP.* ***A.*** *Time from peak 1 to peak 2 in N:C RelA oscillations plotted against IκBα-EGFP fluorescence* ***B.*** *Peak 2 to peak 3 timing.* ***C-D*** *SK-N-AS cells co-expressing RelA-DsRed and either* ***(C.)*** *IκBα-EGFP or* ***(D.)*** *EGFP. Both show peak 1 to peak 2 timing plotted against EGFP fluorescence.*

There was no evidence of a correlation for cells transfected with EGFP or between the timing of peaks 2 to peak 3 and IκBα-EGFP fluorescence. A partial correlation was seen in several experiments between the timing of peaks 1 to peak 2 in HeLa cells or SK-N-AS cells and IκBα-EGFP fluorescence.

Section F: Computational modeling of NF-κB signaling: Analysis of critical variables IκBα and IKK as well as NF-κBα-dependent IκBα transcription (reaction 28). In addition two further critical parameters: IκBα nuclear import rate (reaction 38) and IKK signal onset slow adaptation coefficient (reaction 61) were analysed.

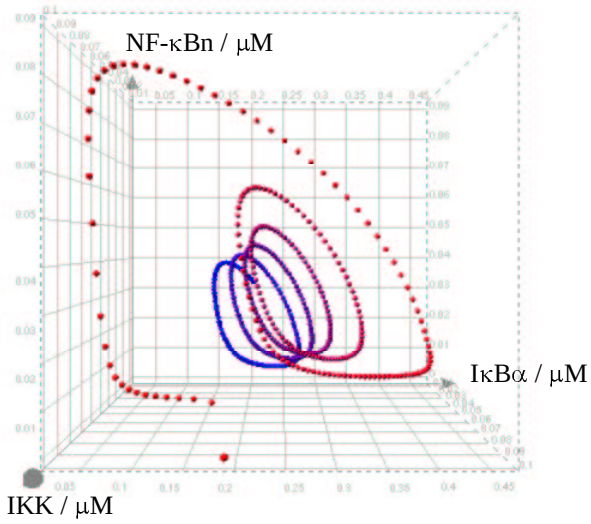

Figure S16: Simple phase plane plot of the time-dependent relationship between the concentrations of IKK, IκBα and nuclear NF-κB using data from the computational model (2). *Time is encoded from red to blue.*

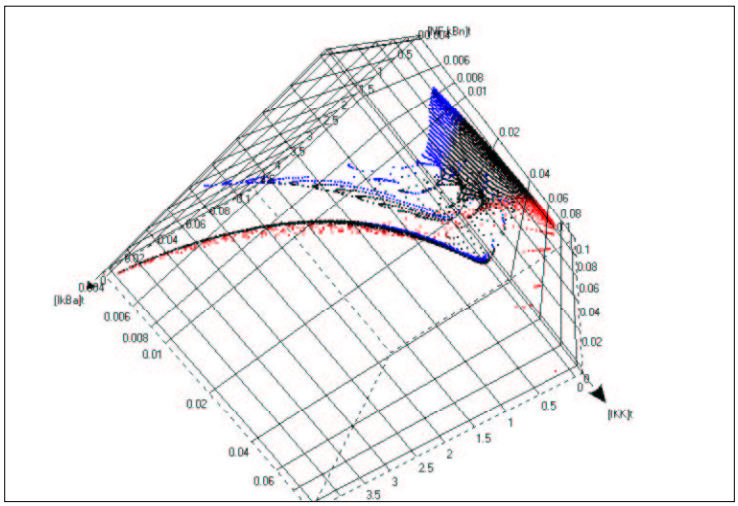

Figure S17. Effect of varying the rate constants for NF-κB dependent IκBα mRNA synthesis (reaction 28) on the phase-plane plot of the co-variation of [nuclear NF-κB], [IκBα] and [IKK]. *Time is encoded from red to blue.*

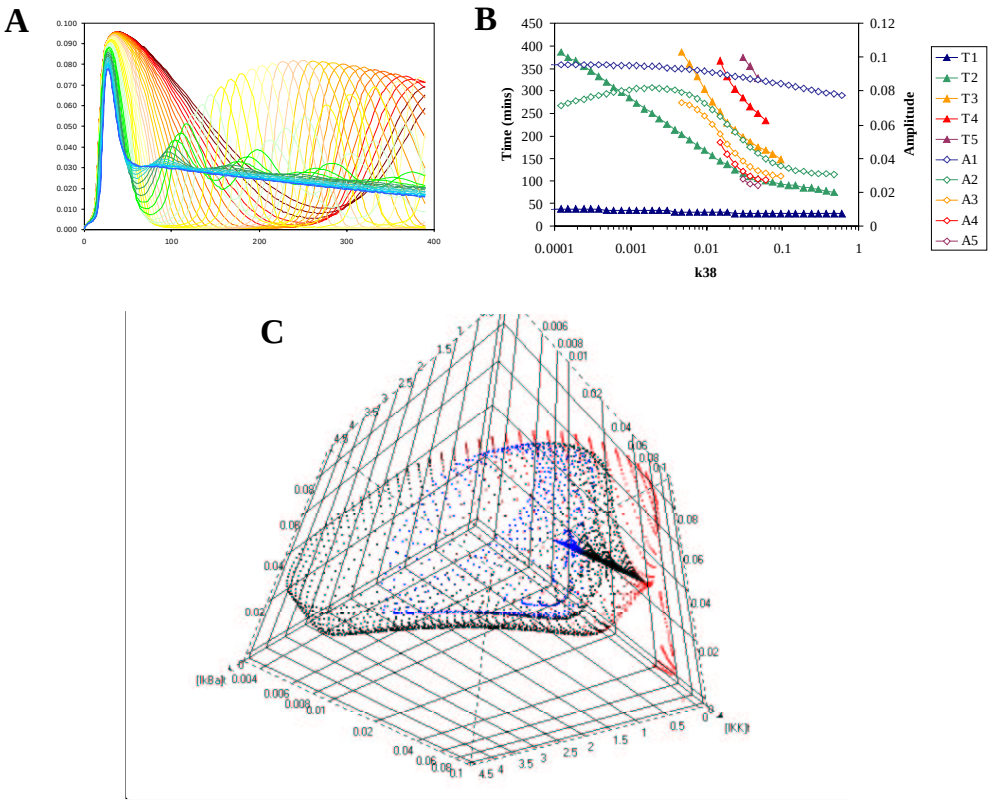

Figure S18. Effect of varying the rate constant for reaction 38 (IκBα nuclear import rate constant) ***A.*** *The simulated time-dependent nuclear localization of NF-κB for successively increasing reaction 38 rate constant two orders of magnitude either side of the standard rate constant is shown by 41 lines changing in regularly increasing log intervals from blue to green to yellow to red (scanned from after equilibration).* ***B.*** *The amplitudes and timings of the simulated peaks for different rate constants (as determined from data in B).* ***C.*** *Phase-plane behavior of IKK, IκBα and free nuclear NF-κB. Time is encoded from red to blue.*

The plots show that oscillations occur only over a narrow range of parameter values.

Increasing rate of IκBα nuclear import tends to shorten the period of the oscillations.

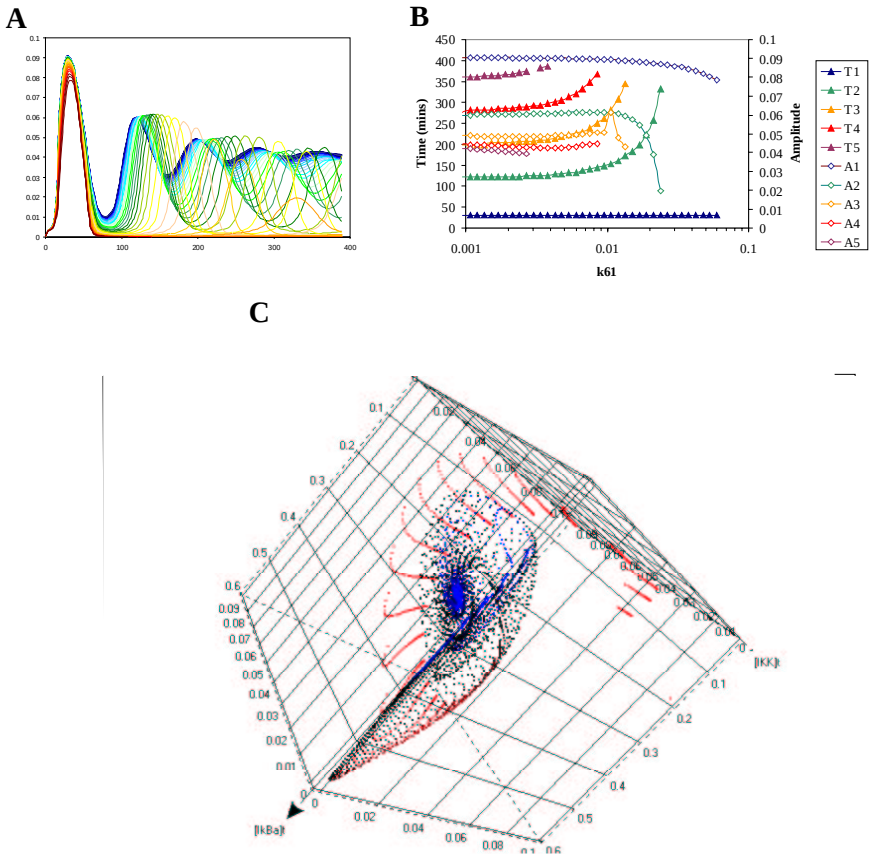

Figure S19. Effect of varying the rate constant for reaction 61 (IKK signal onset slow adaptation coefficient) ***A.*** *The simulated time-dependent nuclear localization of NF-κB for successively increasing reaction 61 rate constant two orders of magnitude either side of the standard rate constant is shown by 41 lines changing in regularly increasing log intervals from blue to green to yellow to red (scanned from after equilibration).* ***B****. The amplitudes and timings of the simulated peaks for different rate constants (as determined from data in B).* ***C.*** *Phase-plane behavior of IKK, IκBα and free nuclear NF-kB. Time is encoded from red to blue.*

This parameter is a measure of the rate of loss of IKK activity. Increases in the rate results in lengthening of period and marked damping of oscillations with successively earlier peaks losing amplitude as the rate is increased.

Section G: Accompanying Videos:

Movie S1: *Time-lapse confocal images of SK-N-AS cells expressing RelA-DsRed (red) and hCMV- IκBα-EGFP (green) over a period of 10 h following continual stimulation with 10 ng/ml TNFα (see Figure 1B and 2A). Images were taken at 3 min intervals.*

Movie S2: *Time-lapse confocal images of SK-N-AS cells expressing RelA-DsRed (red) and EGFP (green) over a period of 10 h following continual stimulation with 10 ng/ml TNFα (see Figure 2C). Images were taken at 3 min intervals.*

Movie S3: *Time-lapse luminescence images of HeLa and SK-N-AS cells expressing pNF-κB-Luc over a period of 25 h after continual stimulation with TNFa (see Figure S11). Images were taken at 30 min intervals (30 min integrations).*

Movie S4: *Time-lapse confocal images of HeLa cells expressing RelA-DsRed-Express and κB-IκBα-EGFP over a period of 15 h following continual stimulation with 10ng/ml TNFα (see Fig. 3A and B). Images were taken at 3 min intervals.*

Supplementary References:

1. G. Nelson *et al., J Cell Sci* **115**, 1137-48 (Mar 15, 2002).
2. A. Hoffmann, A. Levchenko, M. L. Scott, D. Baltimore, *Science* **298**, 1241-5 (Nov 8, 2002).
3. L. Yang, K. Ross, E. E. Qwarnstrom, *J Biol Chem* **278**, 30881-8 (Aug 15, 2003).
4. H. Sakurai, H. Chiba, H. Miyoshi, T. Sugita, W. Toriumi, *J Biol Chem* **274**, 30353-6 (Oct 22, 1999).
5. X. Jiang, N. Takahashi, N. Matsui, T. Tetsuka, T. Okamoto, *J Biol Chem* **278**, 919-26 (Jan 10, 2003).
6. J. A. DiDonato, M. Hayakawa, D. M. Rothwarf, E. Zandi, M. Karin, *Nature* **388**, 548-54 (Aug 7, 1997).